

Filler Materials for Polyphenylenesulphide Composite Coatings

Preprint

Toshifumi Sugama
Brookhaven National Laboratory

Keith Gawlik
National Renewable Energy Laboratory

*To be presented at the GRC 2001 Annual Meeting
San Diego, California
August 26–29, 2001*



NREL

National Renewable Energy Laboratory

1617 Cole Boulevard
Golden, Colorado 80401-3393

NREL is a U.S. Department of Energy Laboratory
Operated by Midwest Research Institute • Battelle • Bechtel

Contract No. DE-AC36-99-GO10337

NOTICE

The submitted manuscript has been offered by an employee of the Midwest Research Institute (MRI), a contractor of the US Government under Contract No. DE-AC36-99GO10337. Accordingly, the US Government and MRI retain a nonexclusive royalty-free license to publish or reproduce the published form of this contribution, or allow others to do so, for US Government purposes.

This report was prepared as an account of work sponsored by an agency of the United States government. Neither the United States government nor any agency thereof, nor any of their employees, makes any warranty, express or implied, or assumes any legal liability or responsibility for the accuracy, completeness, or usefulness of any information, apparatus, product, or process disclosed, or represents that its use would not infringe privately owned rights. Reference herein to any specific commercial product, process, or service by trade name, trademark, manufacturer, or otherwise does not necessarily constitute or imply its endorsement, recommendation, or favoring by the United States government or any agency thereof. The views and opinions of authors expressed herein do not necessarily state or reflect those of the United States government or any agency thereof.

Available electronically at <http://www.doe.gov/bridge>

Available for a processing fee to U.S. Department of Energy
and its contractors, in paper, from:

U.S. Department of Energy
Office of Scientific and Technical Information
P.O. Box 62
Oak Ridge, TN 37831-0062
phone: 865.576.8401
fax: 865.576.5728
email: reports@adonis.osti.gov

Available for sale to the public, in paper, from:

U.S. Department of Commerce
National Technical Information Service
5285 Port Royal Road
Springfield, VA 22161
phone: 800.553.6847
fax: 703.605.6900
email: orders@ntis.fedworld.gov
online ordering: <http://www.ntis.gov/ordering.htm>



Filler Materials for Polyphenylenesulphide Composite Coatings

Toshifumi Sugama
Brookhaven National Laboratory

Keith Gawlik
National Renewable Energy Laboratory

Abstract

Researchers at Brookhaven National Laboratory and the National Renewable Energy Laboratory have tested polymer-based coating systems to reduce the capital equipment and maintenance costs of heat exchangers in corrosive and fouling geothermal environments. These coating systems act as barriers to corrosion to protect low-cost carbon steel tubing; they are formulated to resist wear from hydroblasting and to have high thermal conductivity. Recently, new filler materials have been developed for coating systems that use polyphenylenesulphide as a matrix. These materials include boehmite crystals (orthorhombic aluminum hydroxide, which is grown *in situ* as a product of reaction with the geothermal fluid), which enhance wear and corrosion resistance, and carbon fibers, which improve mechanical, thermal, and corrosion-resistance properties of the composite.

Introduction

Corrosion, erosion, and fouling by scale deposits are major issues for geothermal-fluid-wetted heat exchanger tubes in geothermal power plants at several reservoirs. In some cases, expensive, corrosion-resistant alloys are used in shell and tube heat exchangers because of the need for corrosion resistance. In other cases, frequent heat exchanger retubing is required to repair corroded tube bundles. Capital and maintenance costs of geothermal heat exchangers can be reduced considerably if inexpensive carbon steel tubes could be coated with a low-cost, thermally conductive coating that provides corrosion resistance equal to that of high-grade alloy steels. Scholl (1997) reported that capital costs of a typical geothermal fluid heat exchanger can be reduced 67% if polymer-coated carbon steel tubes, tubesheets, and headers are used in place of titanium tubes and titanium-clad plates. Thus, corrosion-, erosion-, and fouling-resistant coatings for carbon steel tubes are being investigated at Brookhaven National Laboratory (BNL) and the National Renewable Energy Laboratory (NREL), in cooperation with industry partners such as CalEnergy Operating Company, Mammoth Pacific LP, and FPL Energy. These partners have hosted field tests of the coatings at geothermal power plants.

The research program aims to develop a coating less susceptible to high-temperature hydrothermal oxidation. We found that polyphenylenesulfide (PPS) is one polymeric material that could meet these requirements. Although PPS coatings showed oxidation after exposure to acid brine at 200°C, they played a key role in successfully protecting inexpensive carbon steel heat exchanger tubes against corrosion in wet, harsh, geothermal environments (Gawlik et al., 1998, 1999, 2000). Our findings suggested that PPS-coated carbon steel tubes can be used in place of expensive titanium alloys, inconel, and stainless steels, which are frequently used in geothermal power plants. Because of its semicrystalline polymer structure, PPS has good

surface hardness and smoothness. However, when coatings are exposed to brine at 200°C, the surface hardness of hydrothermally oxidized PPS is not high enough to sustain the impact of hydroblasting. In fact, when such surfaces with heavy scale deposits were repeatedly cleaned by hydroblasting, they showed severe wear and tear. The damage was due to the bombardment of hard mineral particles present in the scales during hydroblasting. In the worst case, the coating film was completely worn out, and the underlying steel was corroded. In addition, the PPS coating may not be tough and resilient enough to withstand the bending and impact stresses imposed on the tubes during transportation and installation. Finally, enhancement of the thermal conductivity of the coating would increase heat transfer from the brine and improve plant efficiency.

Ceramics might prove to be good fillers for PPS because of their hardness, excellent wear resistance, and high-temperature stability. Aluminum oxide-rich calcium aluminate (ACA) fillers are of particular interest for coatings in geothermal plants with acidified fluid because they are less susceptible than many other ceramic fillers to reacting unfavorably with hot acid. We investigated the wear rate of ACA-filled and plain PPS, the changes in chemical composition and state of the ACA-filled PPS surfaces after exposure to hot acid brine, the magnitude of the coatings' susceptibility to moisture, and the extent of their uptake of corrosive ionic electrolytes.

Adding carbon fiber to PPS improves both the thermal conductivity of the coating system and its mechanical properties. Barkyoumb et al. (1993) reported that carbon fibers 10-11 μm in diameter have a thermal conductivity ranging from 473 to 809 kcal/hr-m-°C, which is more than six times higher than that of the silicon carbide fillers previously used to improve thermal performance. In addition, carbon fibers have superior tensile strength and elastic modulus. Thus, PPS coatings reinforced with carbon fibers could not only enhance thermal conductivity but also improve mechanical properties.

In field tests at the Mammoth Lakes binary plant, operated by Mammoth Pacific LP, tubes and test coupons coated with ACA-filled PPS are being exposed to production and injection brines. Visual evaluations at the six- and nine-month exposure points have shown that the coatings are completely unaffected by the geothermal fluid. The articles will remain under test for at least a year, when the exposed coatings will be analyzed more comprehensively. FPL Energy has offered to use the ACA-filled PPS coatings in some of their brine/working fluid heat exchangers; preparations for that test are under way.

Experimental Procedures

Test coupons (60 mm x 60 mm) coated with ACA-filled PPS were made in the following manner. Aluminum oxide-rich calcium aluminate was supplied by Lafarge Aluminates. The ACA contained two major chemical constituents: 69.8-72.2% aluminum oxide and 26.8-29.2% calcium oxide. The surface area was 3800-4400 cm^2/g , and the particle size was less than 90 μm . An X-ray powder diffraction (XRD) survey of the ACA revealed that its main mineralogical composition consisted of crystalline calcium dialuminate ($\text{CaO}\cdot 2\text{Al}_2\text{O}_3$) and calcium monoaluminate ($\text{CaO}\cdot \text{Al}_2\text{O}_3$). The metallic substrate used was commercial AISI 1008 carbon steel. A thermoplastic PPS powder with a particle size of less than 60 μm was obtained from Ticona. It had a high melt flow at its melting point, around 240°C. A 45 wt% PPS powder was

mixed with 55 wt% isopropyl alcohol (IPA) to make slurry coatings. The ACA filler at 5, 10, 15, and 20% by weight of the total amount of PPS was then added to the PPS slurry. Before these slurries were deposited on the steel coupons, the coupon surfaces were covered with a zinc phosphate (Zn.Ph) conversion primer by immersing them for 30 min. in a phosphate solution consisting of a 5.0 wt% zinc orthophosphate, 10.0 wt% phosphoric acid, 1.0 wt% manganese (II) nitrate hexahydrate, and 84.0 wt% water at 80°C. Then the Zn.Ph-primed steel surfaces were rinsed with water at 25°C and dried in an oven at 100°C for 30 min. to remove moisture. The crystalline Zn.Ph primer provides cathodic protection of the underlying steel against corrosion and enhances adhesion of the PPS coatings (Sugama, 1994). The primed panels were then dipped into the slurry and withdrawn slowly. The slurry-covered panels were preheated in an air oven at 100°C for one hour to volatilize the alcohol liquid phase and promote the conversion of the slurry into a sintered layer. Then, the sintered layer was heated in air at 320°C for 3 hours, to reach its optimum melt flow, and subsequently cooled to room temperature to make a solid film. This coating process was repeated three times until the thickness of the coating film ranged from 127 to 178 μm .

For the carbon-fiber-filled PPS test coupons, polyacrylonitrile (PAN) precursor-derived carbon fibers $\sim 7.4 \mu\text{m}$ in diameter and $\sim 3 \text{ mm}$ in length, supplied by Asbury Graphite Mills, Inc., were used. The metallic substrate was also commercial AISI 1008 carbon steel primed with Zn.Ph, and the same type of PPS powder was used. Carbon fibers at 0.2, 0.5, 1.0, and 1.5% by weight of the total mass of PPS were added to the PPS slurry. These fiber/PPS slurries were designed to have a similar consistency. Increasing the amount of fiber in the PPS composite necessitated adding more IPA to it to make a slurry of the appropriate consistency. The coating process, similar to the one used above, was repeated three times to obtain a coating film at least 150 μm thick.

Measurements

The coated ACA-filled PPS test panels were exposed for up to 15 days in an autoclave containing a low pH brine solution (1 wt% sulphuric acid, 13 wt% sodium chloride, and 86 wt% water) at 200°C under a hydrothermal pressure of 1.6 MPa. The carbon-fiber-filled PPS test coupons were exposed for up to 14 days in an autoclave containing 20,000 ppm CO_2 -13 wt% NaCl solution at 200°C.

Mechanical and corrosion resistance tests were performed on the ACA-filled PPS test coupons. The sand-blasting wear resistance of the surfaces of exposed and unexposed coatings was assessed using a silica (SiO_2) grit-blasting hand-held gun with a nozzle orifice of 2 mm in diameter. The SiO_2 particles (each about 15 μm) were conveyed by a compressed air pressure of 0.62 MPa from a backpack hopper to the gun. From a standard distance of $\sim 20 \text{ mm}$, the grit was projected for 2 min onto the coating surfaces at an angle of $\sim 45^\circ$. Although the rate of wear in the standard abrasion tests is commonly represented by a loss of mass or volume (Ho, 1997), in this test, the rate was estimated as the depth of wear ($\mu\text{m}/\text{min}$) computed from the difference between the values of surface roughness, R_A (μm), of the coatings before and after the sand-blasting tests. The average roughness was determined by the Profilometer method. X-ray photoelectron spectroscopy (XPS) showed the degree of hydrothermal oxidation and revealed the chemical states formed on the oxidized surfaces of the coatings. The exothermic crystallization

energy of fragments of the coatings removed physically from the underlying steel was investigated by differential scanning calorimetry (DSC) in nitrogen. Alterations in morphological features and elemental distribution of the coating's surfaces and in its profile after exposure were explored using scanning electron microscopy (SEM) and energy-dispersive x-ray spectrometry (EDX). AC electrochemical impedance spectroscopy (EIS) was used to evaluate the ability of the coating films to protect the steel from corrosion. To estimate the protective performance of coatings, the pore resistance, R_p ($\text{ohm}\cdot\text{cm}^2$), was determined from the plateau in Bode-plot scans that occurred in low-frequency regions. Because of space constraints, only the wear resistance and corrosion analyses are described here in detail.

Mechanical, thermal, and corrosion resistance tests were performed on the carbon-fiber-filled PPS coupons. The thickness of the fiber-reinforced and nonreinforced PPS composite coatings deposited on the steel surfaces was determined by the Profilometer method. The thermal conductivity of the reinforced and nonreinforced composite specimens (7.5 cm wide x 13.8 cm long x 1.5 cm high) was measured at room temperature using the Shotherm QTM Thermal Conductivity Meter. Composite coating specimens were prepared to determine mechanical properties, including tensile strength, tensile modulus, and elongation, by casting the composite slurry in dumbbell-shaped molds with a specific gauge length of 31.2 mm, a width of 5.8 mm, and a thickness of 0.8 mm. The cast slurry was then heated for 3 hours at 310°C. An Instron tensile-testing machine was run at a cross-head speed of 2.5 mm/min to obtain the values of mechanical properties, which were reported as the average from three specimens. SEM and EDX were used to explore insights into the detailed microstructure of the composite coating's profile before and after exposure. AC EIS was used to evaluate the ability of the coating films to protect the steel from corrosion. Results for both ACA-filled and carbon-fiber-filled PPS follow, and include wear rates, corrosion resistance, thermal conductivity, and mechanical properties.

Results and Discussion

Results for ACA-filled PPS

Wear rates. Figure 1 shows the changes in the rate of wear by sand blasting for ACA-filled and unfilled PPS coatings as a function of exposure time. For unexposed coatings (denoted as day 0), the rate of wear rises with an increasing amount of ACA filler. Its rate for the bulk PPS without ACA rose ~6.7 times to 0.2 $\mu\text{m}/\text{min}$ when 20 wt% ACA was incorporated into the PPS. One factor causing an increased wear rate is the degree of surface roughness, R_A , of the coatings. R_A is simply the average deviation of a diamond stylus as it traverses the coating from a mathematically constructed center line; it is a true measure of the average height of the asperity. R_A was 0.07, 0.08, 0.09, 0.15, and 0.24 μm for the 0, 5, 10, 15, and 20 wt% ACA-filled coatings. High roughness leading to high wear rates under sand blasting is often seen with other filled coatings, such as PPS/silicon carbide. When the filler particles are eroded by sand blasting, they leave relatively large voids behind on the surface, increasing R_A .

When unfilled PPS was exposed, its wear markedly increased with exposure; its wear rate of 0.93 $\mu\text{m}/\text{min}$ after a 15-day exposure was 30 times higher than that of the unexposed PPS. Thus, the surfaces of exposed PPS coatings appear to become vulnerable to attack from the discharged silica grit, suggesting that PPS is damaged during exposure. In other words, hydrothermal

treatment of PPS at 200°C causes undesirable surface properties, such as a loss of smoothness and less rigidity and hardness. In contrast, there is a dramatic improvement in resistance to blasting wear in all exposed ACA-filled coatings. With 5 wt% ACA, a wear rate of 0.09 $\mu\text{m}/\text{min}$ for unexposed coatings dropped $\sim 44\%$ to 0.05 $\mu\text{m}/\text{min}$ after a 5-day exposure. Prolonging the exposure time to 10 days further improved wear resistance; in fact, the depth of wear was less than 0.01 $\mu\text{m}/\text{min}$. The same results were obtained from the 15-day exposed coatings, implying that ACA fillers greatly reduced the degree of wear in the exposed PPS coatings. Incorporating ACA at levels greater than 10 wt% was better than using 5 wt%; all the coatings containing ACA at more than 10 wt% had a wear depth of less than 0.01 $\mu\text{m}/\text{min}$ after 5 days of exposure. Hence, ACA appears to be a suitable filler for tribologically stressed coatings; it improves surface properties by giving them high rigidity and hardness during exposure. The wear resistance increases with exposure time because ACA is converted *in situ* to crystallized boehmite, an orthorhombic form of aluminum hydroxide which is much harder than the original ACA, as discussed below.

Corrosion resistance. Next, we used AC EIS to evaluate the effectiveness of ACA-filled PPS coatings in protecting the steel substrate from corrosion. On the overall Bode-plot curves [the absolute value of impedance $|Z|$ (ohm-cm²) vs. frequency (Hz)], (not shown), we noted the impedance value in terms of the pore resistance, R_p . This can be determined from the plateau in the Bode plot occurring at a sufficiently low frequency of 5×10^{-2} Hz. Figure 2 plots R_p at 5×10^{-2} Hz for the steel panels coated with the unfilled and ACA-filled PPS as a function of exposure time. For all the unexposed coating panels, R_p ranged from 3×10^{10} to 1×10^{11} . When all the unfilled and filled PPS coating panels except the one with 20 wt% ACA were exposed, R_p gradually fell with increasing exposure time. Since the R_p value reflects the magnitude of ionic conductivity generated by the electrolyte passing through the coating layer, a high R_p value means a low degree of permeation of the electrolytes into the coating films. Hence, extending the exposure time increased the rate of uptake of the electrolytes by these coatings. The data also show that the R_p value of the coating filled with the highest amount of ACA (20 wt%) markedly declined with an elapsed exposure time, from 4.2×10^{10} ohm-cm² before exposure, to 1.8×10^7 ohm-cm² after 15 days of exposure. This finding clearly demonstrates that incorporating an excess amount of ACA enhances the rate of permeation of the electrolytes through the coating. In comparing the R_p values of all the 15-day exposed coatings, we find the effectiveness of the ACA content in ensuring a low degree of permeation of electrolytes to be as follows: 10 wt% > 5 wt% > 0 wt% > 15 wt% > 20 wt% ACA. The coating system most effective in reducing permeability was the 10 wt% ACA-filled coating with a pore resistance of 3×10^{10} ohm-cm², which is 2.3 times higher than that of the bulk PPS coating without ACA.

The results of other analyses (Sugama et al., 2000) to determine the reactions between ACA and the sulfuric acid in the brine indicated that acid brine permeating through the PPS not only leads to the formation of boehmite as the reaction product, it also eliminates calcium from the $\text{CaO} \cdot 2\text{Al}_2\text{O}_3$ and $\text{CaO} \cdot \text{Al}_2\text{O}_3$ phases, the major mineralogical compounds of ACA. A possible interpretation for such depletion of calcium is that the sulphuric acid in brine preferentially reacts with the calcium in the $\text{CaO} \cdot 2\text{Al}_2\text{O}_3$ and $\text{CaO} \cdot \text{Al}_2\text{O}_3$ phases to yield water-soluble calcium sulfate, CaSO_4 . Assuming that the uptake of calcium by sulphuric acid occurs, the water-soluble calcium sulfate might leach out from the coating layer during exposure. The calcium-depleted ACA then provides the amorphous alumina compound. Thus, it appears that the hydrothermal

hydration of alumina led to its phase transformation into crystalline boehmite ($\text{Al}_2\text{O}_3 \cdot \text{H}_2\text{O}$).

Relating this finding to our earlier results indicates that the major contributor to lessening the permeability of oxidized PPS coatings might be the crystalline boehmite derivative formed by the decalcification-hydrothermal hydration reaction of the ACA fillers with a brine containing sulphuric acid. This reaction product formed in the top surface layer not only acted to confer resistance of the coating surfaces to sand-blasting wear, it also reduced the rate of uptake of corrosive electrolytes by the coating. However, *in situ* growth of a substantial amount of reaction product by incorporating excess ACA filler seems to create a porous structure in the coating layers, allowing the electrolytes to permeate easily through the coating.

Results for carbon-fiber-filled PPS

Thermal conductivity. Figure 3 plots thermal conductivity at room temperature for the PPS composites reinforced with different amounts of carbon fibers. The data demonstrated that, although the fibers were multidirectional in the PPS matrix, thermal conductivity tends to increase with an increasing fiber content in the composites. The nonreinforced bulk PPS, the reference samples, had a thermal conductivity of 3.39×10^{-1} kcal/hr-m-°C. When 0.2 wt% fiber was incorporated into the bulk PPS, the value rose 31% to 4.44×10^{-1} kcal/hr-m-°C. A further increase in the fiber content to 1.5 wt% resulted in a twofold increment above that of the nonreinforced PPS. This finding can be taken as evidence that the graphitic basal planes in the carbon fibers play a major role in enhancing the thermal conductivity of the multidirectional fiber-reinforced PPS composites.

Mechanical properties. Since the efficiency of the fiber reinforcement is directly related to the development of high interfacial shear strength at the interfaces between the fibers and the polymer matrix, the ideal interfacial bond should be strong enough to hold the fibers. Yet, at the same time, it should allow a crack to propagate through the matrix without significantly pulling the fibers. This failure mode generates multiple filament fractures, thereby improving the tensile strength of the composites. In contrast, the development of extraordinary bond strength, higher than that of the matrix, leads to a more brittle material. This fragility causes the loss of frictional-stress transfer at the fiber/matrix interfaces, so that cracks propagate through the fibers. This implies that the tensile strength of the composites had become lower, causing a catastrophic failure (Diefendorf, 1985).

Using this information, we investigated mechanical properties, such as tensile strength, tensile modulus, and elongation, for the fiber-reinforced composite films. The results for tensile strength and modulus are shown in Figure 4. The tensile strength of nonreinforced bulk PPS film specimens was 7.9 MPa. As expected, tensile strength was significantly improved by incorporating the fibers into the bulk PPS films. In this test series, the 1.5 wt% fiber-reinforced film specimens displayed the highest tensile strength, 32.2 MPa, a more than fourfold improvement over that of the plain PPS. A similar tendency toward an increase in strength with an increasing amount of fiber was observed from the tensile modulus, which was computed from the initial slope of the tensile stress-strain curve. Elongation measurements taken during tensile failure indicated that the fibers in the PPS matrix aid the composite films in straining elastically. In fact, 1.5 wt% fiber reinforcement allowed as much as a 5% elongation.

Relating these findings to SEM image analysis of the fiber surfaces, we assumed that numerous gutters, or longitudinal grooves, found on the fiber surfaces may serve to anchor them in the PPS matrix, conferring a good mechanical interlocking bond at the fiber/PPS interfaces. To support this, a polished cross-sectional area of the 0.5 wt% fiber-reinforced composite films was explored using SEM. The SEM image revealed a microstructure in which the fiber was embedded into the PPS matrix. No segregation of the fibers from the matrix was evident in the micrograph, suggesting that the surfaces of the fibers adhere adequately to the matrix. Figure 5 shows the SEM micrograph coupled with the EDX spectrum of the fracture surfaces of the composite films after a tensile test. The fractograph clearly displayed that the entire surfaces of the fibers being pulled out from the matrix phase were covered with matrix materials. Correspondingly, the EDX spectrum taken from the materials clinging to the fiber's surfaces showed sulphur as the dominant element, reflecting the coverage of PPS over the surfaces. Thus, the main failure took place through the PPS matrix. One contributor to this failure mode is the mechanical interlocking bond developed at the critical interfacial boundary zone between the PPS and the rough fiber surfaces. The other possible contributor is the chemical affinity of the PPS for the carbonyl functional groups existing at the outermost surface of the fibers. This affinity might be enough to enhance the fiber reinforcement efficiency, thereby establishing an interfacial shear strength that generates frictional-stress transfer between the fibers and the matrix. Hence, we believe that interfacial mechanical bonds are one of the major factors in improving the mechanical properties of fiber-reinforced PPS composite films.

Corrosion resistance. Corrosion resistance was explored in a manner similar to that used for the ACA-filled PPS coupons. EIS tests were conducted on the panels coated with the 0, 0.2, 0.5, 1.0, and 1.5 wt% fiber-reinforced PPS composites before and after exposure in the autoclave. The thickness of these composite coatings was, respectively, 170, 170, 160, 110, and 60 μm ; increasing the amount of fiber decreased the thickness of the coating films. Incorporating more fibers into the slurry used for coating required lowering the proportion of PPS to IPA to obtain a slurry of the appropriate consistency. This reduction explains why the coating films became thinner as the fiber content increased. Before exposure, R_p of the nonreinforced coating specimens was 4.5×10^{10} ohm-cm², as shown in Figure 6. When the PPS coating film was reinforced with 0.2 wt% fibers, the value increased to 6.4×10^{10} ohm-cm². A further increase in R_p was found for the 0.5 wt% fiber-reinforced films, suggesting that incorporating fibers into the PPS matrix lowers ion permeability. The fibers seem to make the film's microstructure more dense. However, at 1.0 wt%, R_p fell by one order of magnitude to 7.0×10^9 ohm-cm², compared with that of the 0.5 wt% fiber specimens, and R_p declined further in the 1.5 wt% fiber-reinforced coating film. One possible reason for the declining R_p is the thinness of the film formed when less than 1 wt% fiber was incorporated into the PPS. Although there is no experimental evidence, another reason may be that air was trapped by the fibers during mixing into the PPS slurry. Trapped air in the slurry may cause a porous microstructure to form. Over the 14 days of exposure, R_p of all the coating specimens tended to decline, implying that prolonged exposure caused the uptake of more electrolytes by the coating layers. Nevertheless, 0.5 wt% seemed the most effective amount of fiber to minimize the rate of penetration of electrolytes into the composite layers, and this composite coating retained an R_p of $\sim 10^{10}$ ohm-cm² after the 14-day exposure.

SEM micrographs coupled with EDX spectra for a polished cross-sectional area of the steel panel coated with 0.5% fiber-reinforced PPS after 14 days of exposure were used to determine if corrosion occurred on the steel surface. The SEM analysis showed no sign of corrosion-related damage to the underlying steel. In addition, the micrographs showed the outstanding adherence of the reinforced PPS to the Zn.Ph primer. Hence, the 0.5 wt% fiber-reinforced PPS coatings appear to confer sufficient protection to the underlying steel against corrosion in the CO₂-laden brine at 200°C.

Conclusions

Additives to PPS can increase wear resistance when ACA is used and improve the thermal conductivity and mechanical properties when carbon fibers are added. Both fillers better protect the underlying steel from corrosion, in comparison to plain PPS. The *in situ* growth of crystalline boehmite, derived from ACA during exposure to acidified brine, reinforced the oxidized PPS and contributed significantly to improving the coating's resistance to sand-blasting wear. The formation of a combined surface layer of PPS with boehmite reduced the rate of uptake of electrolyte by the coatings, compared with that of the oxidized PPS without ACA, ensuring better protection of the underlying steel against corrosion. A carbon fiber content of 0.5 wt% was the most effective amount to minimize the rate of penetration of electrolytes through the composite film layers. Furthermore, the multidirectional fibers in the composites contributed significantly to enhancing their thermal conductivity and to improving the mechanical properties of the coating films.

References

- Barkyoumb, J.H., Land, D.J., and Kidder, J.N., 1993, "Thermal Conductivity of Single Carbon Fibers Using Photothermal Deflection Techniques," *Material Research Society Symposium Proceedings*, vol. 305, p. 117.
- Diefendorf, R.J., 1985, "The Chemical Nature of the Fiber/Resin Interface in Composite Materilas," in *Tough Composite Materials* [Vosteen, L.E., et al., eds.], Noyes Publications, New Jersey, p. 191.
- Gawlik, K., Sugama, T., Webster, R., and Reams, W., Sept. 22-23, 1998, "Field Testing of Heat Exchanger Tube Coatings," *Geothermal Resources Council Transactions*, vol. 22, pp. 385-391.
- Gawlik, K., Kelley, S., Sugama, T., Webster, R., and Reams, W., Oct. 17-20, 1999, "Field Testing of Heat Exchanger Tube Coatings," *Geothermal Resources Council Transactions*, vol. 23, pp. 65-69.
- Gawlik, K., Sugama, T., Webster, R., and Reams, W., 2000, "Development and Field Testing of Polymer Heat Exchanger Tube Coatings," *Geothermal Resources Council Transactions*, vol. 24.
- Ho, C.T., 1997, "Wear of Carbon Fiber-Reinforced Tin-Lead Alloy Composites," *Journal of Material Science*, vol. 16, p. 1767.

Scholl, K., July 1, 1997, "Report on Liner Application/Heat Exchanger Construction Techniques," National Renewable Energy Laboratory, NREL Milestone Report 2.2.3.

Sugama, T., and Caciello, N.R., 1994, "Interfaces of Polyphenylenesulphide (PPS) Coated Zinc Phosphated Steels After Heating-Cooling Cycles in a Wet, Harsh Environment," *Journal of Coating Technology*, vol. 66, p. 45.

Sugama, T., and Hayenga, P., 2000, "Boehmite-reinforced Poly(phenylene sulphide) as a Wear/Corrosion Resistant Coating," *Polymers & Polymer Composites*, vol. 8, no. 5, pp. 307-318.

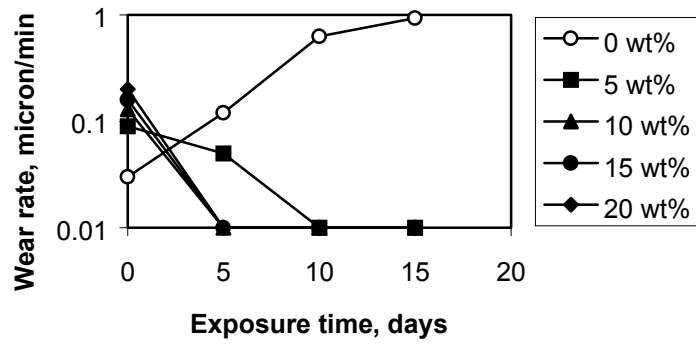


Figure 1. Wear rates for ACA-filled and unfilled PPS.

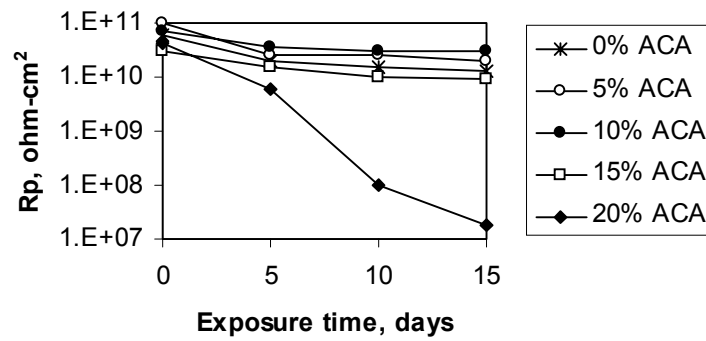


Figure 2. Changes in pore resistance for ACA-filled and unfilled PPS.

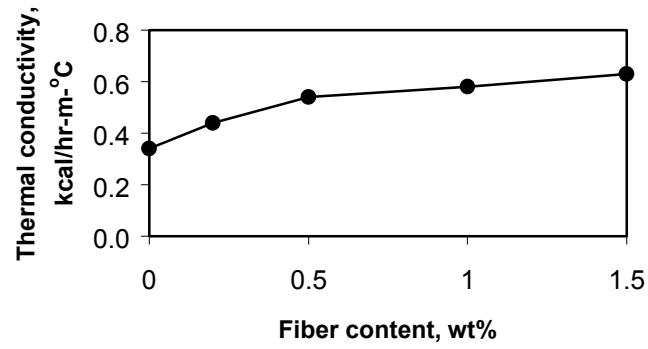


Figure 3. Thermal conductivity of carbon-fiber-filled PPS.

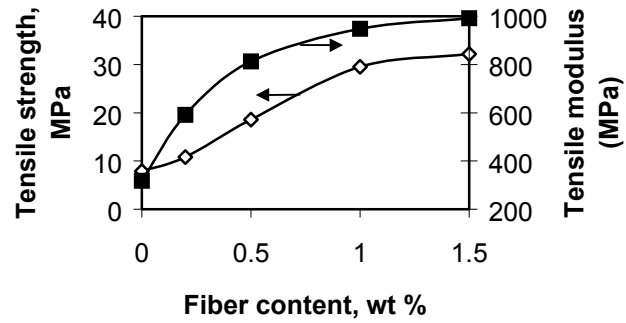


Figure 4. Mechanical properties of carbon-fiber-filled PPS.

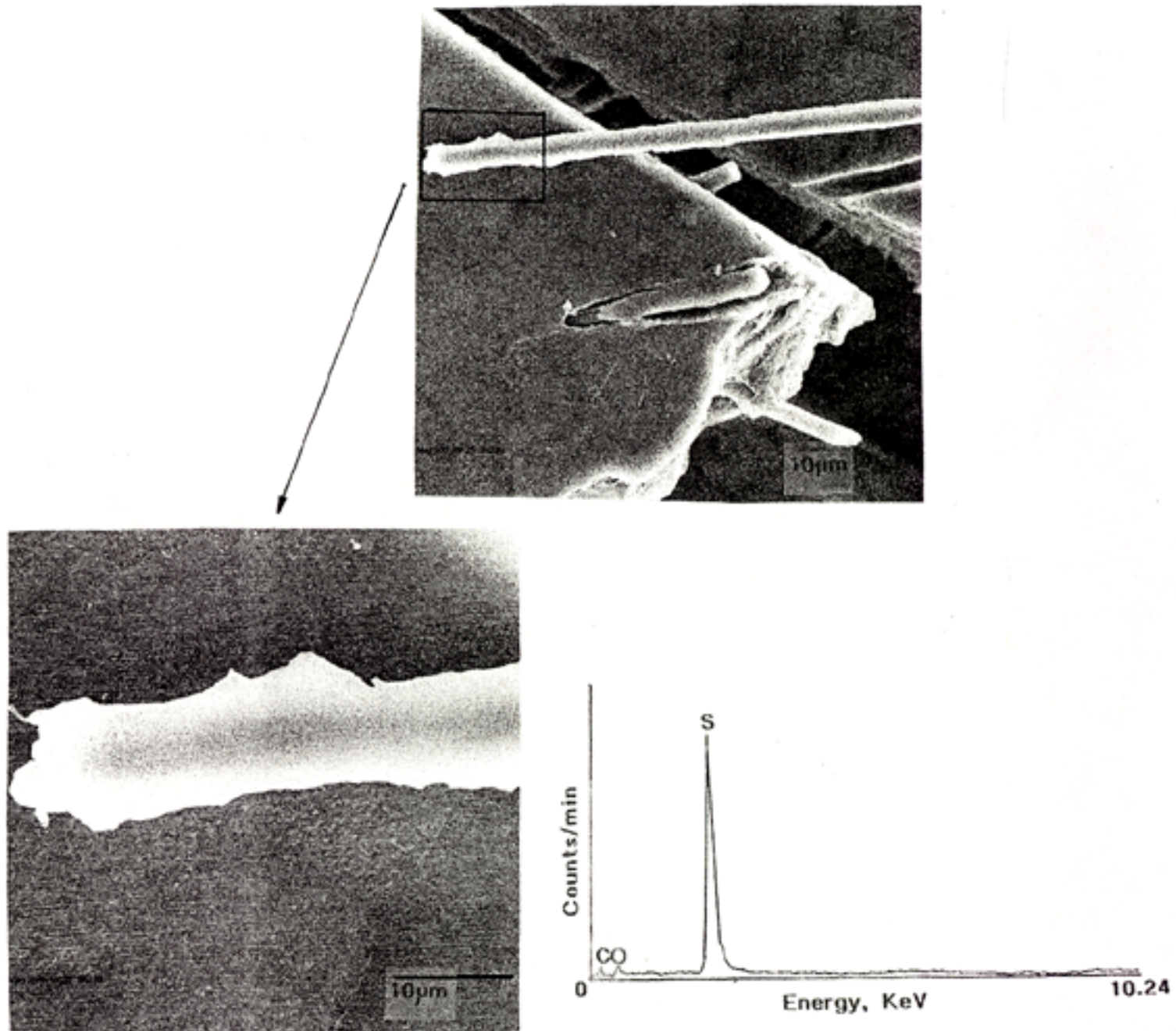


Figure 5. SEM micrograph coupled with EDX spectrum for fractured surfaces of fiber-reinforced PPS composite film after tensile test

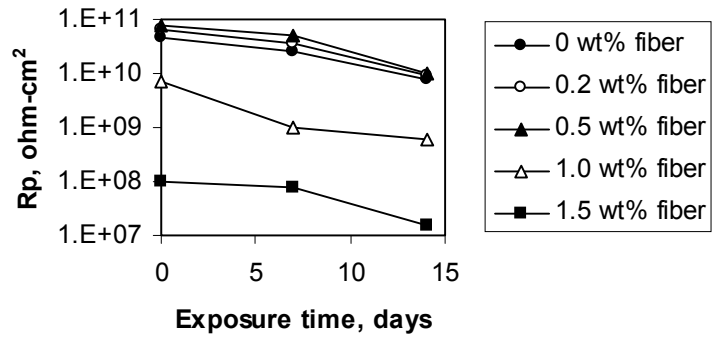


Figure 6. Pore resistance of carbon-fiber-filled PPS.

REPORT DOCUMENTATION PAGE			Form Approved OMB NO. 0704-0188
Public reporting burden for this collection of information is estimated to average 1 hour per response, including the time for reviewing instructions, searching existing data sources, gathering and maintaining the data needed, and completing and reviewing the collection of information. Send comments regarding this burden estimate or any other aspect of this collection of information, including suggestions for reducing this burden, to Washington Headquarters Services, Directorate for Information Operations and Reports, 1215 Jefferson Davis Highway, Suite 1204, Arlington, VA 22202-4302, and to the Office of Management and Budget, Paperwork Reduction Project (0704-0188), Washington, DC 20503.			
1. AGENCY USE ONLY (Leave blank)	2. REPORT DATE June 2001	3. REPORT TYPE AND DATES COVERED Conference paper	
4. TITLE AND SUBTITLE Filler Materials for Polyphenylenesulphide Composite Coatings			5. FUNDING NUMBERS GT11.1107
6. AUTHOR(S) Toshifumi Sugama and Keith Gawlik			
7. PERFORMING ORGANIZATION NAME(S) AND ADDRESS(ES)			8. PERFORMING ORGANIZATION REPORT NUMBER NREL/CP-550-30258
9. SPONSORING/MONITORING AGENCY NAME(S) AND ADDRESS(ES) National Renewable Energy Laboratory 1617 Cole Blvd. Golden, CO 80401-3393			10. SPONSORING/MONITORING AGENCY REPORT NUMBER
11. SUPPLEMENTARY NOTES NREL Technical Monitor: NA			
12a. DISTRIBUTION/AVAILABILITY STATEMENT National Technical Information Service U.S. Department of Commerce 5285 Port Royal Road Springfield, VA 22161			12b. DISTRIBUTION CODE
13. ABSTRACT (<i>Maximum 200 words</i>) Researchers at Brookhaven National Laboratory and the National Renewable Energy Laboratory have tested polymer-based coating systems to reduce the capital equipment and maintenance costs of heat exchangers in corrosive and fouling geothermal environments. These coating systems act as barriers to corrosion to protect low-cost carbon steel tubing; they are formulated to resist wear from hydroblasting and to have high thermal conductivity. Recently, new filler materials have been developed for coating systems that use polyphenylenesulphide as a matrix. These materials include boehmite crystals (orthorhombic aluminum hydroxide, which is grown <i>in situ</i> as a product of reaction with the geothermal fluid), which enhance wear and corrosion resistance, and carbon fibers, which improve mechanical, thermal, and corrosion-resistance properties of the composite.			
14. SUBJECT TERMS Polymer-based coatings; filler materials; polyphenylenesulphide composites			15. NUMBER OF PAGES
			16. PRICE CODE
17. SECURITY CLASSIFICATION OF REPORT Unclassified	18. SECURITY CLASSIFICATION OF THIS PAGE Unclassified	19. SECURITY CLASSIFICATION OF ABSTRACT Unclassified	20. LIMITATION OF ABSTRACT UL